

# Oxalate Oxidase for In Situ H<sub>2</sub>O<sub>2</sub>-generation in Unspecific Peroxygenase-Catalysed Drug Oxyfunctionalisations

Elvira Romero,<sup>[a]</sup> Magnus J. Johansson,<sup>[b]</sup> Jared Cartwright,<sup>[c]</sup> Gideon Grogan<sup>[d]</sup> and Martin A. Hayes<sup>\*[a]</sup>

- 
- [a] Dr. E. Romero, Prof. M. A. Hayes  
Compound Synthesis and Management, Discovery Sciences  
BioPharmaceuticals R&D, AstraZeneca  
Pepparedsleden 1, SE-431 83, Mölndal (Sweden)  
E-mail: martin.hayes@astrazeneca.com
- [b] Prof. M. J. Johansson  
Medicinal Chemistry, Research and Early Development, Cardiovascular, Renal and Metabolism (CVRM)  
BioPharmaceuticals R&D, AstraZeneca  
Pepparedsleden 1, SE-431 83, Mölndal (Sweden)  
and  
Department of Organic Chemistry  
Stockholm University  
Svante Arrhenius väg 16C, SE-106 91, Stockholm (Sweden)
- [c] Dr. J. Cartwright  
Department of Biology  
University of York  
Heslington, York YO10 5DD (United Kingdom)
- [d] Prof. G. Grogan  
Department of Chemistry  
University of York  
Heslington, York YO10 5DD (United Kingdom)

**Abstract:** H<sub>2</sub>O<sub>2</sub>-driven enzymes are of great interest for industrial biotransformations. Herein, we show for the first time that oxalate oxidase (OXO) is an efficient *in situ* source of H<sub>2</sub>O<sub>2</sub> for one of these biocatalysts, which is known as unspecific peroxygenase (UPO). OXO is reasonably robust, produces only CO<sub>2</sub> as a by-product and uses oxalate as a cheap sacrificial electron donor. UPO is a top-rated catalyst for selective C-H oxyfunctionalisations, as we confirm herein by testing a diverse drug panel using miniaturised high-throughput assays and mass spectrometry. 33 out of 64 drugs were converted in 5 µL-scale reactions by the UPO with OXO (conversion >70% for 11 drugs). Furthermore, 84% isolated yield was achieved for the drug tolmetin on a larger scale (50 mg, TON<sub>UPO</sub> 25,664), which was excelled by implementing enzyme immobilization. This one-pot approach ensures adequate H<sub>2</sub>O<sub>2</sub> levels, enabling rapid access to industrially relevant molecules which are difficult to obtain by other routes.

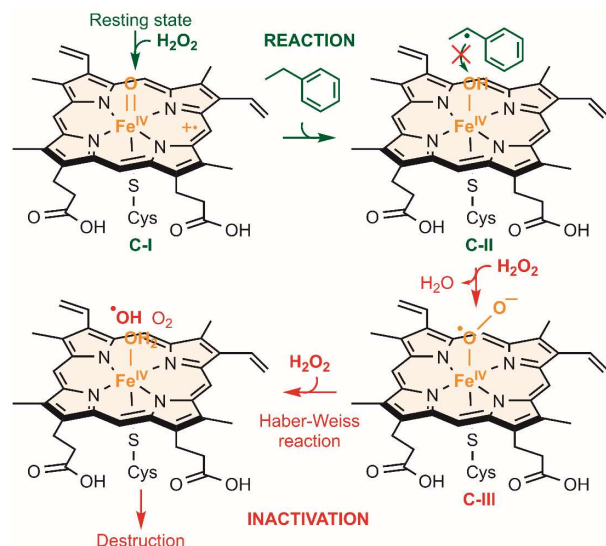
Enzymes are gaining increasing importance in industrial synthetic chemistry.<sup>[1]</sup> They often exhibit excellent selectivity, high catalytic efficiency under mild-reaction conditions and deliver reduced amounts of by-products, in contrast to traditional chemical catalysts. However, the full potential of enzyme-catalysed synthesis in industry is yet to be exploited. Among oxidoreductases, hydrogen peroxide (H<sub>2</sub>O<sub>2</sub>)-driven enzymes exhibit various advantages in industrial processes, compared to other enzymes which require expensive cofactors such as NADPH.<sup>[2]</sup> H<sub>2</sub>O<sub>2</sub> is a powerful oxidizing agent that is cheap, relatively safe and only produces water as a by-product. Oxidoreductases that use H<sub>2</sub>O<sub>2</sub> as an electron acceptor include unspecific peroxygenases (UPOs, EC 1.11.2.1). These enzymes, which incorporate one oxygen atom from H<sub>2</sub>O<sub>2</sub> into the reaction product, have attracted much attention over the past decade. UPOs catalyse C-H oxyfunctionalisations of a wide variety of

industrially relevant molecules, offering advantages over their transition metal catalyst counterparts in terms of selectivity and sustainability.<sup>[3]</sup> UPOs and cytochromes P450 (P450, EC 1.14.14.1) catalyse similar reactions, but UPOs are more robust and do not require expensive cofactors or redox partners.<sup>[4]</sup>

Implementation of UPOs in industrial synthesis would be significantly facilitated by more effective approaches to supply adequate levels of H<sub>2</sub>O<sub>2</sub> in the reactions.<sup>[2]</sup> Excessive levels of H<sub>2</sub>O<sub>2</sub> lead to irreversible inactivation of the UPO by heme destruction (**Scheme 1**). To overcome this, H<sub>2</sub>O<sub>2</sub> can be slowly added to the reactions using a syringe pump or in aliquots. However, *in situ* H<sub>2</sub>O<sub>2</sub>-production improves the green metrics which are used to evaluate the sustainability of industrial chemical processes.<sup>[1a]</sup> This is due to the fact that the palladium-catalysed anthraquinone process, which is generally used for large-scale manufacture of H<sub>2</sub>O<sub>2</sub>, is not environmentally friendly.<sup>[5]</sup>

Numerous *in situ* H<sub>2</sub>O<sub>2</sub>-generation systems have been investigated to mitigate UPO inactivation that involve chemical, electrochemical, photochemical, photoelectrochemical, photoenzymatic, mechanical or enzymatic strategies.<sup>[4, 6]</sup> The most frequent drawbacks for non-enzyme based technologies are production of hydroxyl radicals, substrate overoxidation, low turnover number, complex reactors/procedures, high energy input, undesired by-products or photocatalyst photobleaching (**Table S1**). Oxidase-based H<sub>2</sub>O<sub>2</sub>-generation systems have therefore attracted a great deal of attention because they are user-friendly, cost-effective and sustainable (**Scheme 2**). Among these, the implementation of formate oxidase (FOX, EC 1.2.3.1) is especially interesting since it only produces CO<sub>2</sub> as a by-product,<sup>[7]</sup> but a more robust FOX with a lower *K<sub>m</sub>* is desired.<sup>[7a]</sup> Inspired by the studies on FOX, we show here for the first time that oxalate oxidase (OXO, EC 1.2.3.4)<sup>[8]</sup> is an efficient alternative as an H<sub>2</sub>O<sub>2</sub>-source for the C-H oxyfunctionalisation reactions catalysed by UPOs. Currently, OXO is used to determine plasma and urine

oxalate (1) levels,<sup>[9]</sup> to produce transgenic crops with an increased oxalate tolerance<sup>[10]</sup> and in biofuel cells.<sup>[11]</sup> Using high-throughput liquid handling and mass spectroscopy, we have determined the influence of various parameters on UPO and OXO reactions at  $\mu\text{L}$ -scale and then identified the products for diverse pharmaceutically relevant substrates using UPLC-QTOF/MS<sup>E</sup> data. In addition, we successfully upscaled one these reactions. These studies demonstrate that OXO serves as an efficient  $\text{H}_2\text{O}_2$ -generation system adding high value to the rapidly-increasing toolbox for industrial biotechnology.

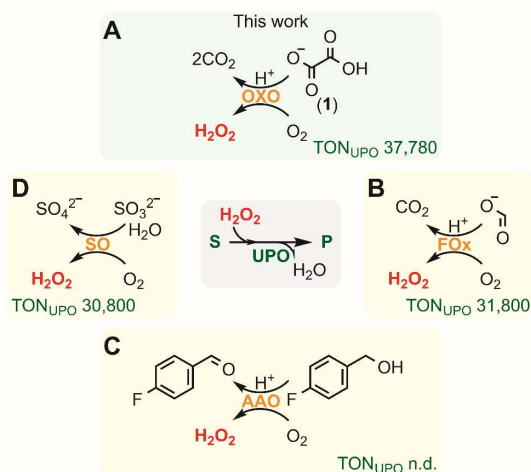


**Scheme 1.**  $\text{H}_2\text{O}_2$ -driven PaDa-I inactivation. C-II reacts with  $\text{H}_2\text{O}_2$  to form C-III instead of reacting with an organic substrate. Next, reaction between C-III and  $\text{H}_2\text{O}_2$  yields hydroxyl radicals which hydroxylate the heme.<sup>[12]</sup>

Previous studies showed that *H. vulgare* (barley) OXO (HvOXO) is very resistant to heat and proteases and can be expressed in yeast.<sup>[8b]</sup> This prompted us to select HvOXO for our  $\text{H}_2\text{O}_2$ -generation system. In the present study, HvOXO was produced by fermentation of *Komagataella phaffii* (*Pichia pastoris*) and purified using Ni-sepharose resin (Fig. S2). To assess the efficiency of the HvOXO-oxalate system for  $\text{H}_2\text{O}_2$ -generation, the previously studied *Agroclybe aegerita* UPO (AaeUPO) variant, known as PaDa-I,<sup>[13]</sup> was used in all C-H oxyfunctionalisations. Expression and purification of PaDa-I were performed following similar protocols to those previously described (Fig. S2).<sup>[14]</sup>

After producing both enzymes, we compared their stability and pH optima to assess their compatibility. First, their melting temperature ( $T_m$ ) was determined by the ThermoFluor method (Fig. 1 and S3). HvOXO  $T_m$  values were higher than  $50^\circ\text{C}$  at all assayed pHs and its long-term stability was also satisfactory (Fig. S4). Higher thermostability was similarly observed for PaDa-I at pH 4.0 and 5.0, though PaDa-I was more rapidly inactivated at pH 3.0 (Fig. S4). Next, we studied the influence of pH on the kinetic parameters for HvOXO.  $k_{\text{cat}}$  and  $K_m(\text{oxalate})$  values increased 3- and 244-fold as the pH rose from 3.0 to 5.0, respectively (Table 1, Fig. S5-6). These studies also showed that HvOXO exhibits strong substrate inhibition at pH 3.0, but not at pH 4.0 so this was the preferred pH for HvOXO reactions. Conveniently, the optimal pH

of PaDa-I for activity is usually slightly acidic, but varies depending on the substrate.<sup>[13]</sup>



**Scheme 2.** *In situ* oxidase-based  $\text{H}_2\text{O}_2$ -generation systems. For UPO-catalysed conversion of ethylbenzene (S) into (*R*)-1-phenylethanol (P),  $\text{TON}_{\text{UPO}}$  values ( $\mu\text{mol product}/\mu\text{mol UPO}$ ) are indicated. AAO, aryl-alcohol oxidase (EC 1.1.3.7)<sup>[15]</sup>; SO, sulfite oxidase (EC 1.8.3.1)<sup>[16]</sup>; n.d., not determined.

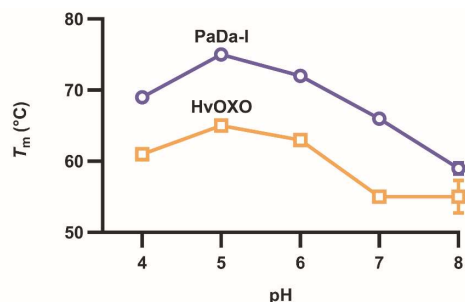


**Figure 1.**  $T_m$  values of PaDa-I (●) and HvOXO (□). Note that error bars are too small for visualization in some instances in all figures.

**Table 1.** Steady-state kinetic parameters of HvOXO using oxalate.<sup>[a]</sup>

pH	$k_{\text{cat}}$ [ $\text{s}^{-1}$ ]	$K_m$ [mM]	$k_{\text{cat}}/K_m$ [ $\text{mM}^{-1}\text{s}^{-1}$ ]
3	$0.57 \pm 0.03$	$0.09 \pm 0.02$	$6.33 \pm 1.45$
4	$1.52 \pm 0.05$	$0.73 \pm 0.09$	$2.08 \pm 0.27$
5	$1.87 \pm 0.04$	$22.00 \pm 1.67$	$0.09 \pm 0.01$

[a] Reactions contained  $0.025 \mu\text{M}$  HvOXO,  $0.125 \mu\text{M}$  PaDa-I,  $0.03$ - $200 \text{ mM}$  oxalate,  $0.07 \text{ mM}$  MBTH and  $1 \text{ mM}$  DMAB in air-saturated  $100 \text{ mM}$  buffer at  $25^\circ\text{C}$ .

Reactions containing PaDa-I, HvOXO and oxalate were first tested using ethylbenzene (2) as a model substrate, which gives the products (*R*)-1-phenylethanol (3) and acetophenone (4)<sup>[17]</sup> (Fig. 2). In parallel, the drug tolmetin (5) was assayed as a PaDa-I substrate to start investigating the potential of combining these enzymes for late-stage functionalisation of bioactive compounds. Full conversion after 24 h was observed for the ethylbenzene,

while almost 25% conversion was achieved with tolmetin (**5**). The  $\text{TON}_{\text{UPD}}$  for ethylbenzene was a little higher (37,780) than that reported for the top-rated oxidase-based  $\text{H}_2\text{O}_2$ -generation systems (**Scheme 2**).

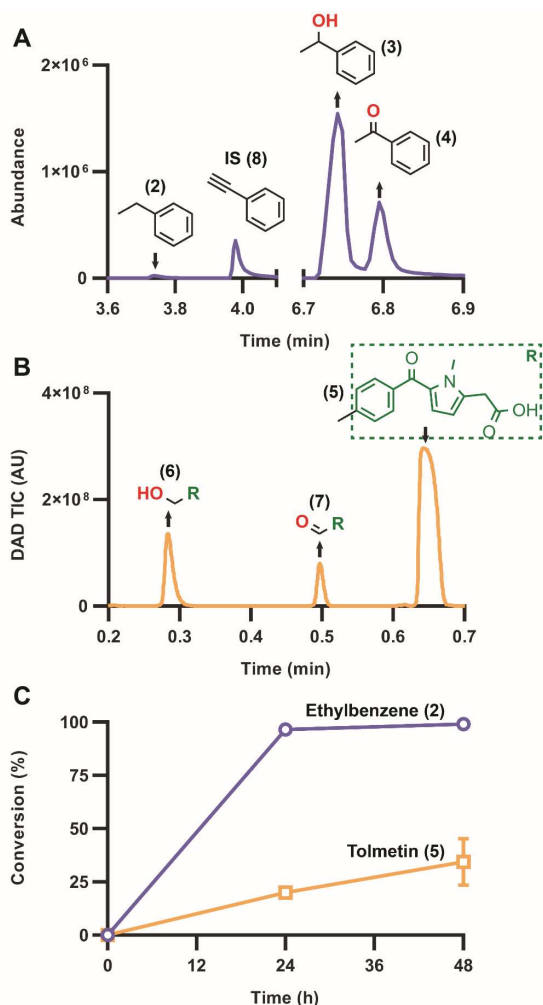


**Figure 2.** PaDa-I-catalysed conversion of ethylbenzene (**A, C, ●**) and tolmetin (**B, C, ◻**). Reactions (100  $\mu\text{L}$ ) contained 1  $\mu\text{M}$  PaDa-I, 1  $\mu\text{M}$  HvOXO, 50 mM ethylbenzene or tolmetin, 200 mM oxalate, 200 mM buffer at pH 5.0. Analyses after 24 (**A, B**) and 48 h at 1000 rpm. Reactions with ethylbenzene and tolmetin contained 10 and 5% acetonitrile, respectively. 100% dioxygen gas was blown for 5 min in the empty 3 mL vials, placed on ice, before the addition of the reaction components. **IS (8)**, internal standard.

Subsequently, the drug tolmetin (**5**) was used as a model substrate to study the influence of various parameters on  $\mu\text{L}$ -scale reactions containing PaDa-I and HvOXO. First, increasing HvOXO concentrations were tested (**Fig. S7-8**). At pH 3.0 and 4.0, an equimolar concentration of HvOXO and PaDa-I was optimal. Contrarily, a 3-fold higher HvOXO:PaDa-I ratio was required at pH 5.0 to obtain the same conversion as that observed for the reactions containing 10 mM  $\text{H}_2\text{O}_2$  instead of HvOXO-oxalate. This is due to the fact that HvOXO exhibits a high  $K_{\text{m(oxalate)}}$  at pH 5.0 (**Table 1**) and thus a higher oxalate concentration is recommended at this pH.

Next, we used an equimolar concentration of HvOXO and PaDa-I at pH 4.0 to further study the efficiency of their partnership. Reactions containing low tolmetin and  $\text{H}_2\text{O}_2$  concentrations (without HvOXO) led to full conversions after 2 h (**Fig. S9A**). The same outcome was observed when  $\text{H}_2\text{O}_2$  was replaced with HvOXO and oxalate, only with extended incubation times due to the slow release of  $\text{H}_2\text{O}_2$ . However, the HvOXO-oxalate system is advantageous for reactions which contain higher tolmetin concentrations (**Fig. 3**). A single addition of an equivalent  $\text{H}_2\text{O}_2$  concentration (10 mM) resulted in around 2.6-fold less product than when using HvOXO after 20.5 h. Only in the case of reactions with a single addition of  $\text{H}_2\text{O}_2$ , conversions were similar after 2 and 20.5 h due to PaDa-I inactivation (**Fig. S9B**).

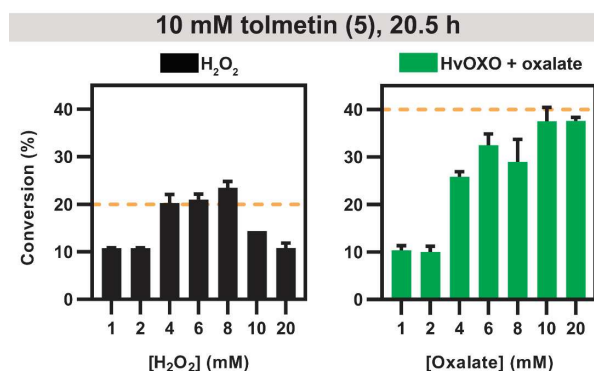


**Figure 3.** PaDa-I-catalysed conversion of tolmetin with  $\text{H}_2\text{O}_2$  or HvOXO. Reactions (5  $\mu\text{L}$ ) contained 0.1  $\mu\text{M}$  PaDa-I, 0 or 0.1  $\mu\text{M}$  HvOXO, 1-20 mM  $\text{H}_2\text{O}_2$  or oxalate, buffer at pH 4.0 and 24% dimethyl sulfoxide.

The influence of twelve co-solvents on tolmetin conversion was also investigated, since they are often needed for substrate solubilization. In reactions with 10% co-solvent and HvOXO, conversions were higher than 75% in the presence of glycerol, acetonitrile, acetone or tetrahydrofuran (**Fig. 4**). In reactions with 25% co-solvent (**Fig. S10B**), only glycerol was well-tolerated by HvOXO. In contrast, reactions initiated by a single  $\text{H}_2\text{O}_2$  addition were not influenced by 25% acetonitrile, which was the best cosolvent for PaDa-I. Thus, the best option for reactions with both PaDa-I and HvOXO is 10% acetonitrile. Similarly, we tested various temperatures (25-50  $^\circ\text{C}$ ) for the reactions containing these enzymes, which indicated that a temperature of 25  $^\circ\text{C}$  is optimal (**Fig. S11**).

Subsequently, acetonitrile was selected for a more difficult challenge with up to 100 mM tolmetin. Results using HvOXO with 10-100 mM oxalate were compared to those for the same reactions with 10-100 mM  $\text{H}_2\text{O}_2$  (**Fig. 5** and **S12**). As expected, PaDa-I was rapidly inactivated at high  $\text{H}_2\text{O}_2$  concentrations. In reactions containing 100 mM both tolmetin and oxalate, a  $\text{TON}_{\text{UPD}}$  of 71,377 was determined after 20.5 h. The outcome of these experiments clearly demonstrated the benefits of using HvOXO when high substrate loadings are required.

These results encouraged us to upscale the tolmetin (**5**) conversion (from 0.1 mg/5  $\mu\text{L}$  to 50 mg/7.5 mL). Resulting products **6**, **7** and **9** (**Fig. 6**) were separated by HPLC and identified by NMR (**Section S1.13** and **S2.2**, **Fig. S13-15**). In parallel, an identical reaction was performed with cross-linked enzyme aggregates containing both PaDa-I and HvOXO (combi-CLEA, **Fig. 6** and **S16-17**, **Section S1.12-13**.) instead of using

the soluble enzymes. 84 and 100% isolated yield was achieved for the reaction containing the soluble enzymes ( $TON_{UPO}$  25,664) and the combi-CLEA ( $TON_{UPO}$  30,699), respectively. In the case of the combi-CLEA reaction, enzymes were active for longer time to mainly yield product **9**.

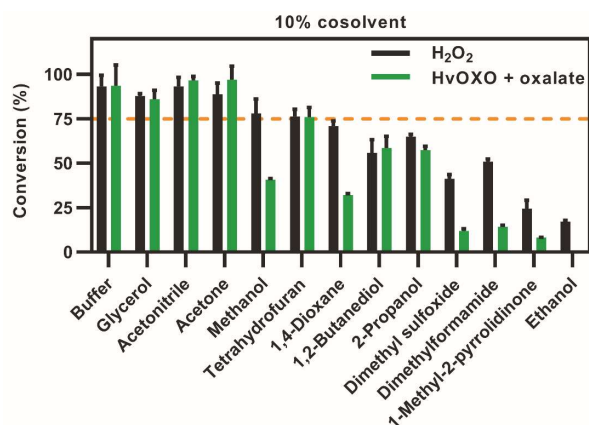


**Figure 4.** Influence of cosolvents on PaDa-I reactions with  $H_2O_2$  or HvOXO. Reactions (5  $\mu$ L) contained 0.1  $\mu$ M PaDa-I, 0 or 0.1  $\mu$ M HvOXO, 0.5 mM tolmetin, 2 mM oxalate or  $H_2O_2$ , buffer at pH 4.0. Analyses after 20.5 h.

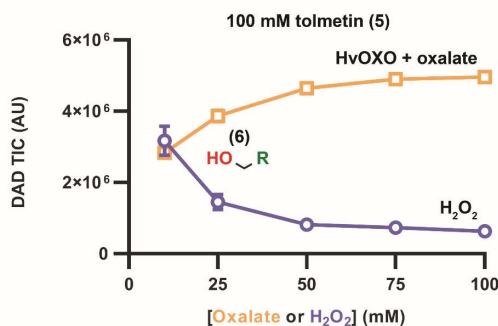


**Figure 5.** PaDa-I-catalysed conversion of 100 mM tolmetin with  $H_2O_2$  or HvOXO. Reactions (5  $\mu$ L) contained 0.1  $\mu$ M PaDa-I, 0 or 0.1  $\mu$ M HvOXO, buffer at pH 4.0 and 11% acetonitrile. Analyses after 20.5 h. Peak areas for product **6** are plot. Those for product **7** are shown in Fig. S12.

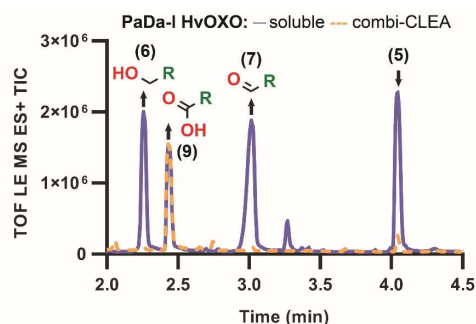


**Figure 6.** PaDa-I-catalysed conversion of 50 mg tolmetin (26 mM) with HvOXO. Reactions (7.5 mL) contained 0.8  $\mu$ M PaDa-I, 0.8  $\mu$ M HvOXO, 168 mM oxalate, buffer at pH 5.0. Analyses after 96 h.

After performing the reaction optimization and upscaling using tolmetin, we demonstrated the great PaDa-I capability for late-stage modification of a diverse drug panel using the HvOXO-oxalate system in 5  $\mu$ L reactions. 33 out of 64 drugs were used as a substrate by PaDa-I, with conversions of 2-100% (Fig. 7 and S18). The corresponding UPLC-QTOF/MS<sup>E</sup> data were used to tentatively identify major reaction products for various high conversion reactions (Section S2.3). In the case of empagliflozin (**12**), oxidation on the tetrahydrofuran ring likely produced compound **75** which was followed by ring opening to form a carboxylic acid product (**76**). PaDa-I presumably accomplished the aromatic mono-hydroxylation of methotrimeprazine (**14**) and triflupromazine (**15**), while this enzyme found two oxidation sites on the indole ring of fluvastatin (**86**). Phenylbutazone (**23**) was likely hydroxylated by PaDa-I on the butyl side chain (**87**). In the clozapine (**18**) reaction, a dihydroxylated dechlorinated clozapine-*N*-oxide (**81**) and a hydroxylated clozapine-*N*-oxide (**82**) seemed to be the main products. Formation of a product with an aliphatic *N*-oxide (**85**) likely occurred using 5-benzyloxygramine (**21**) as a PaDa-I substrate. In the ketoconazole reaction, one of the main products was presumably *O*-dealkylated ketoconazole (**83**). In the case of raloxifene (**20**), our results suggested that PaDa-I peroxidative activity (Scheme S1) might have yielded substrate radicals which were subjected to non-enzymatic formation of a covalent raloxifene homodimer (**84**). These results confirm the extraordinary ability of PaDa-I to enable various types of oxygenation reactions and one-electron oxidations of non-native substrates.<sup>[18]</sup>

In summary, we demonstrated here that HvOXO can play an important role as a  $H_2O_2$ -source in the UPOs oxyfunctionalisations using an inexpensive sacrificial electron donor. Furthermore, this work showed for the first time that it is possible to do high-throughput screening using 5  $\mu$ L-scale UPO reactions by converting 33 drugs, while reaction upscaling (50 mg) was achieved as well. HvOXO is fairly robust, although enhancing its cosolvent tolerance may be beneficial for g-scale reactions, which is in progress in order to unlock its full potential in diverse sustainable industrial processes.

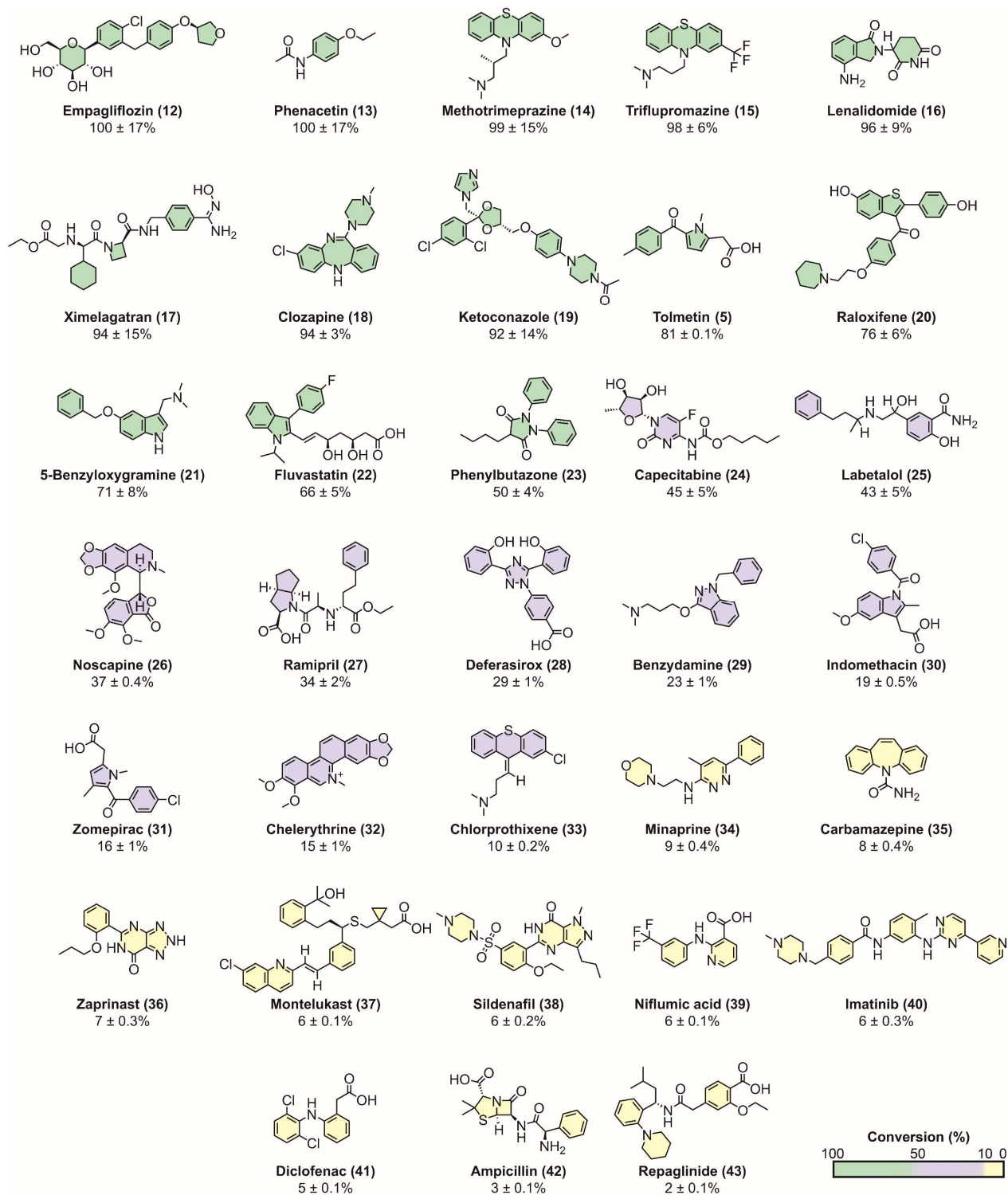


**Figure 7.** Drugs converted by PaDa-I. All reactions (5  $\mu$ L) contained 0.8  $\mu$ M PaDa-I, 0.8  $\mu$ M HvOXO, 0.5 mM drug, 10 mM oxalate, buffer at pH 4.0, 2.5% either acetonitrile or tetrahydrofuran (**Table S2**). Conversions (%) after 24 h are indicated.

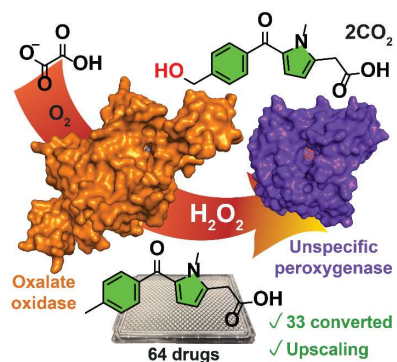
## Acknowledgements

The authors thank Dr. Ileana Guzzetti for her help with NMR and Stefan Blaho for training in fermentations.

**Keywords:** Biocatalysis • High-throughput screening • H<sub>2</sub>O<sub>2</sub>-generation • oxidoreductases • drug late-stage functionalisation

- [1] a) E. L. Bell, W. Finnigan, S. P. France, A. P. Green, M. A. Hayes, L. J. Hepworth, S. L. Lovelock, H. Niikura, S. Osuna, E. Romero, K. S. Ryan, N. J. Turner, S. L. Flitsch, *Nat. Rev. Methods Primers* **2021**, *1*, 1-21; b) S. Wu, R. Snajdrova, J. C. Moore, K. Baldenius, U. Bornscheuer, *Angew. Chem. Int. Ed.* **2020**, *59*, 2-34.
- [2] B. O. Burek, S. Bormann, F. Hollmann, J. Z. Bloh, D. Holtmann, *Green Chem.* **2019**, *21*.
- [3] Y. Wang, D. Lan, R. Durrani, F. Hollmann, *Curr. Opin. Chem. Biol.* **2017**, *37*, 1-9.
- [4] G. Grogan, *JACS Au* **2021**, *1*, 1312-1329.
- [5] a) J. M. Campos - Martin, G. Blanco - Brieve, J. L. G. Fierro, *Angew. Chem. Int. Ed.* **2006**, *45*, 6962-6984; b) C. Xia, Y. Xia, P. Zhu, L. Fan, H. Wang, *Science* **2019**, *366*, 226-231.
- [6] M. Hobisch, D. Holtmann, P. G. de Santos, M. Alcalde, F. Hollmann, S. Kara, *Biotechnol. Adv.* **2021**, *51*, 1-13.
- [7] a) F. Tieves, S. J. P. Willot, M. M. C. H. van Schie, M. C. R. Rauch, S. H. H. Younes, W. Zhang, J. Dong, P. Gomez de Santos, J. M. Robbins, B. Bommarius, M. Alcalde, A. S. Bommarius, F. Hollmann, *Angew. Chem. Int. Ed.* **2019**, *58*, 7873-7877; b) S. J.-P. Willot, M. D. Hoang, C. E. Paul, M. Alcalde, I. W. C. E. Arends, A. S. Bommarius, B. Bommarius, F. Hollmann, *ChemCatChem* **2020**, *12*, 2713-2716.
- [8] a) M. Sugiura, H. Yamamura, K. Hirano, M. Sasaki, M. Morikawa, M. Tsuboi, *Chem. Pharm. Bull.* **1979**, *27*, 2003-2007; b) M. M. Whittaker, J. W. Whittaker, *J. Biol. Inorg. Chem.* **2002**, *7*, 136-145.
- [9] F. Hong, N.-O. Nilvebrant, L. J. Jönsson, *Biosens. Bioelectron.* **2003**, *18*, 1173-1181.
- [10] D. M. Livingstone, J. L. Hampton, P. M. Phipps, E. A. Grabau, *Plant Physiol.* **2005**, *137*, 1354-1362.
- [11] a) S. Xu, S. D. Minteer, *ACS Catal.* **2012**, *2*, 91-94; b) D. P. Hickey, M. S. McCammant, F. Giroud, M. S. Sigman, S. D. Minteer, *J. Am. Chem. Soc.* **2014**, *136*, 15917-15920.
- [12] A. Karich, K. Scheibner, R. Ullrich, M. Hofrichter, *J. Mol. Catal. B Enzym.* **2016**, *134*, 238-246.
- [13] P. Molina-Espeja, E. Garcia-Ruiz, D. Gonzalez-Perez, R. Ullrich, M. Hofrichter, M. Alcalde, *Appl. Environ. Microbiol.* **2014**, *80*, 3496-3507.
- [14] P. Molina-Espeja, S. Ma, D. M. Mate, R. Ludwig, M. Alcalde, *Enzymes Microb. Technol.* **2015**, *73*, 29-33.
- [15] P. Gomez de Santos, S. Lazaro, J. Viña-Gonzalez, M. D. Hoang, I. Sánchez-Moreno, A. Glieder, F. Hollmann, M. Alcalde, *ACS Catal.* **2020**, *10*, 13524-13534.
- [16] M. M. C. H. van Schie, A. T. Kaczmarek, F. Tieves, P. Gomez de Santos, C. E. Paul, I. W. C. E. Arends, M. Alcalde, G. Schwarz, F. Hollmann, *ChemCatChem* **2020**, *12*, 3186-3189.
- [17] M. Kluge, R. Ullrich, K. Scheibner, M. Hofrichter, *Green Chem.* **2012**, *14*, 440-446.
- [18] M. Hofrichter, H. Kellner, R. Herzog, A. Karich, J. Kiebig, K. Scheibner, R. Ullrich, *Antioxidants* **2022**, *11*, 163.

## Entry for the Table of Contents



**Unspecific peroxygenase has a new partner!** High-throughput  $\mu\text{L}$ -scale screenings revealed optimal conditions for *in situ*  $\text{H}_2\text{O}_2$ -generation using oxalate oxidase. This enzymatic tandem exhibits extraordinary potential for selective C-H oxyfunctionalisation reactions of complex drug scaffolds.

Institute and/or researcher Twitter usernames: @AstraZeneca, @UniOfYork, @ElvRomGuz